PHYSICAL REVIEW B **72**, 060407(R) (2005)

Magnetic phase diagram of the colossal magnetoelectric $DyMn_2O_5$

W. Ratcliff II,[1] V. Kiryukhin,[2] M. Kenzelmann,[1,3] S.-H. Lee,[4] R. Erwin,[1] J. Schefer,[5] N. Hur,[2] S. Park,[2] and S-W. Cheong[2]
[1]*NIST Center for Neutron Research, National Institute of Standards and Technology, Gaithersburg, Maryland 20899, USA*
[2]*Department of Physics and Astronomy, Rutgers University, Piscataway, New Jersey 08854, USA*
[3]*Department of Physics and Astronomy, The Johns Hopkins University, Baltimore, Maryland 21218, USA*
[4]*Department of Physics, University of Virginia, Charlottesville, Virginia 22904, USA*
[5]*Laboratory for Neutron Scattering ETHZ and PSI, CH-5232 Villigen PSI, Switzerland*
(Received 13 April 2005; published 25 August 2005)

We report neutron-diffraction measurements of the magnetic phase diagram of the colossal magnetoelectric $DyMn_2O_5$. Our measurements reveal the magnetic origin of the complex dielectric anomalies in this material. Frustrated magnetic interactions result in a large density of low-energy magnetic states which can be selected by the application of relatively small magnetic fields. The unusual combination of magnetic frustration and strong magnetoelastic coupling is responsible for the remarkable changes of the dielectric properties of $DyMn_2O_5$ in small applied magnetic fields.

DOI: 10.1103/PhysRevB.72.060407 PACS number(s): 75.80.+q, 75.25.+z, 77.80.−e

Materials exhibiting strong coupling between magnetic and dielectric properties, the magnetoelectrics, have been studied for many decades because of the technologically important possibility of controlling the dielectric properties using a magnetic field.[1–3] Unfortunately, compounds showing large magnetoelectric (ME) effects are extremely rare. Recent discoveries of giant ME effects in $REMnO_3$ and $REMn_2O_5$ (*RE* is Tb, Ho, or Dy) have led to a dramatic renaissance in the field.[4–7] The microscopic origin of the effects of a magnetic field on the dielectric constant and polarization in these materials have not yet been revealed. To elucidate this origin, it is necessary to understand the relationship between the magnetic structure and the dielectric properties. In this paper, we report neutron-diffraction measurements of the magnetic phase diagram of $DyMn_2O_5$. The dielectric constant and the spontaneous electric polarization of this compound exhibit complex anomalous behavior as the temperature and the magnetic field are varied.[7] Our measurements reveal the microscopic properties of the magnetic transitions in this material, and establish the magnetic origin of the dielectric anomalies. They also help to show why the giant ME effect in $DyMn_2O_5$ occurs in relatively small magnetic fields.

$DyMn_2O_5$ crystallizes in the orthorhombic *Pbam* structure.[8] The structure consists of edge-sharing $Mn^{4+}O_6$ octahedra forming chains along the *c* axis. These chains are crosslinked via $Mn^{3+}O_5$ pyramidal units.[8] Magnetic interactions in the Mn subsystem are geometrically frustrated,[9] and $DyMn_2O_5$ shows a complicated series of magnetic transitions involving the Mn and Dy ions on cooling below $T \approx 42$ K. (Refs. 9 and 10). For $T > 8$ K, the magnetic ordering wave vector is of the form $q=[0.5,0,0.25+\delta(T)]$ where δ is small. This ordering primarily involves the Mn spins, although there is also a small contribution from the Dy moments.[9,10] For $T < 8$ K, additional magnetic peaks ("the Dy peaks") associated with ordering of the Dy sublattice, but also having a contribution from Mn, appear at $q=(0.5,0,0)$. $DyMn_2O_5$ undergoes a transition to a ferroelectric (FE) phase at $T_c \approx 40$ K with the spontaneous polarization appearing along the *b* axis.[7,11] For the isostructural $TbMn_2O_5$ and YMn_2O_5 compounds, it was proposed that the FE state exhibits canted antiferroelectric displacements of the Mn^{3+} ions.[9,12] These displacements are expected to lift the magnetic degeneracy by lowering the crystal symmetry to $Pb2_1m$, thus stabilizing the FE state via the magnetic Jahn-Teller effect.[13] However, the actual structure of the FE state is unknown at this time.

We report on single-crystal neutron-diffraction studies of the magnetic phase diagram of $DyMn_2O_5$. We find that the anomalies in the dielectric constant and the electric polarization in this compound are correlated with magnetic transitions, and we establish the magnetic character of the phases involved. We find that with changing temperature or magnetic field, a series of strongly hysteretic transitions between magnetic states takes place. The complexity of the dielectric properties of $DyMn_2O_5$ stems from the complexity of the magnetic phase diagram. Frustrated magnetic interactions between the Mn ions, and the magnetic coupling of the large Dy moments to the Mn subsystem, give rise to several different magnetic states, which can be selected by application of relatively small magnetic fields. Therefore, magnetic frustration, the presence of many low-energy magnetic states, and strong spin-lattice coupling are the key factors explaining the giant magnetoelectric properties of $DyMn_2O_5$.

A $DyMn_2O_5$ single crystal was grown using $PbO—PbF_2$ flux in a Pt crucible. The crystal volume was ~ 65 mm^3. Elastic neutron-scattering measurements were performed using the SPINS cold neutron triple-axis spectrometer at the NIST Center for Neutron Research. The spectrometer configuration was guide-Be-80′-S-80′-D at an energy of 5 meV. The sample was mounted in a vertical-field superconducting magnet. The crystal was aligned such that the $(h,2h,l)$ zone coincided with the horizontal scattering plane. In $DyMn_2O_5$, the largest ME effects are observed when the magnetic field is applied along the *a* axis of the crystal.[7] In our experimental configuration, $\sim 90\%$ of the magnetic field is applied along the *a* axis. Some data were also taken in the $(h,0,l)$ scattering plane in zero magnetic field. To determine the magnetic structure, ~ 300 magnetic Bragg peaks were mea-

sured using the 4-circle TRICS instrument at the SINQ facility at the Paul Scherrer Institute.

There are two main magnetic phases in $DyMn_2O_5$. One phase is a low-temperature ($T<8$ K) antiferromagnetic (AFM) state with $q=(0.5,0,0)$. Its structure was recently determined at 2 K by Blake *et al.*[9] The other is a spiral phase with $q=(0.5,0,0.25+\delta)$ present for $T<42$ K. To characterize the magnetic order of the spiral phase, we measured magnetic Bragg peaks at $T=22$ K on cooling from the paramagnetic phase. At this temperature, the spiral phase is commensurate ($\delta=0$). Best fits with $\chi^2=2$ were found for a magnetic structure with the following moments: $Mn^{3+}:1.6(2)\mu_B$, $Mn^{4+}:1.5(2)\mu_B$, and $Dy^{3+}:1.2(3)\mu_B$. Neighboring Mn^{3+} spins were found to be antiferromagnetically aligned, and the Mn^{4+} spins were found to spiral along the c axis with a phase factor $e^{2\pi i(0.25d)}$, where d is the distance between neighboring Mn^{4+} ions along the c axis. The Dy moments point close to the b axis, with a Dy pair lying on the perpendicular bisector of a Mn^{3+} pair having antiparallel spins. This structure shares similarities to the $q=(0.5,0,0)$ structure at 2 K found by Blake *et al.*,[9] which has no modulation along the c axis. While for the Mn^{3+} ions, the modulation simply rotates the spins from one unit cell to the next along the c axis, the Mn^{4+} spins in one unit cell are no longer ferromagnetic at 22 K but rotate continuously from one Mn^{4+} site to the next. This means there are no longer zigzag Mn^{3+}/Mn^{4+} antiferromagnetic spin chains along the a axis. The spiral on the Mn^{4+} spins gives further evidence that interactions between the Mn spins in $DyMn_2O_5$ are frustrated.[9] As a function of temperature and field, the wave vector of the spiral changes. As in other magnetic systems, these changes may reflect the system's attempt to relieve some of the frustration.

Figure 1(a) shows the temperature dependence of the dielectric constant on cooling and warming. The large peak at $T\approx38$ K (cooling) is due to the transition to the FE state. The lowest-temperature anomaly coincides with the appearance of the $q=(0.5,0,0)$ magnetic ordering vector and the full ordering of the Dy moments.[7] To relate the dielectric anomalies to magnetic transitions, we have measured the temperature dependence of four magnetic peaks of the $(0.5,0,0.25+\delta)$ type, and of the (0.5,1,0) and (0.5,1,1) Dy peaks. The temperature dependences of the intensity and the wave vectors of the $(0.5,1,1.25+\delta)$ and the (0.5,1,1) peaks taken on warming and on cooling are shown in Figs. 1(b) and 1(c), respectively. At the lowest temperature, coexisting peaks with two different values of δ, $\delta=0$ and $\delta=-0.015$, are present. We refer to these two magnetic states, one commensurate and the other incommensurate, as the C and the $IC1$ state, respectively. As the temperature is raised, the $q=(0.5,0,0)$ order vanishes abruptly at $T=7.5$ K. Simultaneously, anomalies appear in the intensities of the C and $IC1$ peaks, revealing a spin-reorientation transition.[14] These transitions correlate with the abrupt increase in the dielectric constant shown in Fig. 1(a). As the temperature is raised further, the value of δ in the $IC1$ state begins to rise towards zero. For $T>10$ K, the wave vector of the C phase deviates from its low-temperature commensurate value, and δ becomes positive. We call this incommensurate state with $\delta>0$ the $IC2$ state to distinguish it from the $IC1$ state, in which δ is negative. At $T=18$ K, there is a lock-in transition, at which the value of δ of the $IC1$ state reaches zero and the C state reemerges. At approximately the same temperature, the wave vector of the $IC2$ state locks in at $\delta=0.015$. In addition, a spin-reorientation transition occurs at this temperature. These changes correlate with a peak in the dielectric constant seen in Fig. 1(a). As the temperature continues to rise, the intensity of the $IC2$ peak decreases, until the $IC2$ phase disappears almost completely at $T\approx27$ K. At the same temperature, another spin reorientation occurs in the C state, and a sharp anomaly is seen in the dielectric constant. At $T\approx37$ K, an incommensurate state reappears, in coexistence with the C state. Finally, at $T\approx42$ K, long-range magnetic order is lost.

On cooling, the C state dominates for $10\text{ K}<T<38$ K. There is a spin reorientation and the associated dielectric anomaly at $T\approx27$ K. At $T\approx19$ K, the intensities of the $IC2$ peaks begin to rise significantly. There is another spin reorientation in the C state at $T\approx15$ K. It correlates with a clear increase of the dielectric constant. At $T\approx10$ K the $IC1$ state appears. The $IC1$ state undergoes a spin reorientation at $T=6.5$ K. Finally, the $q=(0.5,0,0)$ peaks appear at $T=5.5$ K, simultaneously with a drop in the dielectric constant. Summarizing, the data of Fig. 1 show that the dielectric anomalies in $DyMn_2O_5$ have their origin in the transitions between the various magnetic states in this compound.

We now turn to the effects of a magnetic field. Figure 2 shows contour maps of the intensity of the $(0.5,1,1.25+\delta)$ peaks at different temperatures as the field is ramped up, then down. Application of the field at $T=4.2$ K [Fig. 2(a)] results in the destruction of the $IC1$ state in a field slightly exceeding $H=2$ T. The magnetic field initially stabilizes the C state, which undergoes two spin reorientations as the field increases. However, at ~4 T the C state disappears; it is replaced by an incommensurate state with $\delta>0$ (the $IC2$ state). As the field is reduced from its highest value of 6 T, the $IC2$ state remains locked at $\delta=0.03$ until the field reaches ~3 T. At lower fields, the $IC2$ wave vector gradually decreases, until the C and the $IC1$ states reappear for $H<2$ T [Fig. 2(b)]. Figures 2(c) and 2(d) show the effects of the field at 15 K (upon warming, after heating to 60 K, then cooling to 4.2 K). The zero-field C state is replaced by the $IC2$ state at $H\approx4$ T. On ramping the field down, the $IC2$ state persists down to zero field, even though the value of δ decreases for $H<2$ T. Finally, at $T=30$ K, where only the C state is present, the magnetic structure is not affected by the fields achievable in our experiments, see Figs. 2(e) and 2(f).

In $DyMn_2O_5$, the ME effects are most pronounced at the lowest temperatures.[7,11] The data of Figs. 2(a) and 2(b) show that the magnetic state at these temperatures is quite complex. In addition to the peaks shown in Fig. 2, the $q=(0.5,0,0)$ magnetic peaks are present at $T=4.2$ K. To elucidate the relationship of the dielectric properties to the magnetic structure in this important temperature region, we plot the magnetic-field dependences of the electric polarization (magnetic field parallel to a), and the intensities of the (0.5,1,1) and (0.5,1,1.25) peaks in Fig. 3. The intensity at the nuclear peak position (1,2,0), reflecting the ferromagnetic contribution, is also shown. To be directly comparable with

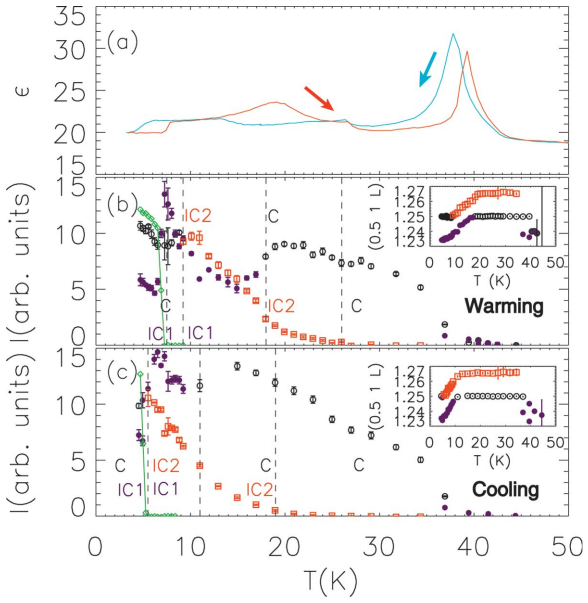

FIG. 1. (Color) Temperature dependence of the dielectric constant on warming and cooling (a). T dependence of the intensities of the (0.5,1,1) and $(0.5,1,1.25+\delta)$ peaks on warming (b), and cooling (c). The insets show the corresponding changes of the reciprocal space position of the latter peak. Black symbols denote the C ($\delta=0$), blue—the $IC1$ ($\delta<0$), and red—the $IC2$ ($\delta>0$) phases. Green symbols show the intensity of the (0.5,1,1) peak.

the polarization, the neutron data of Fig. 3 are shown versus the a-axis component of the applied field H_a, as the b component of the field has only a minor effect on the dielectric properties.[7] As the field is increased, the intensity of the magnetic peaks remains flat initially, probably because of single-ion anisotropy. At $H_a \approx 1.2$ T, there is a spin reorientation (spin flop) of the Dy spins evidenced by the drop of the intensity of the (0.5,1,1) peak. The $q=(0.5,0,0.25)$ C state also undergoes a spin reorientation at this field, likely driven by the reorientation of the Dy spins. As H_a is increased to ~1.9 T, the $IC1$ state vanishes (see Fig. 2), and the intensity of the Dy peaks begins to decrease. At a slightly larger field intensity appears on the (1,2,0) nuclear peak, which is indicative of spin canting. A further increase of the field to $H_a \approx 2.4$ T results in the disappearance of the (0.5,0,0) and an increase in the intensity of the C peak. At higher fields, the C peak intensity decreases, and the C-$IC2$ transition occurs at $H_a \approx 4.1$ T. The observed magnetic transitions can be correlated with the anomalies in the electric polarization of Fig. 3(a). The first drop in the polarization appears to be associated with the disappearance of the $IC1$ state and with the beginning of the spin canting. The second and, perhaps, the third coincide with the suppression of the $q=(0.5,0,0)$ magnetic peaks. The subsequent changes are associated with the evolution of the C state. The differences between the exact transition fields of the magnetic and the dielectric transitions are likely due to the different measurement conditions, as described in the experimental part, and sample dependency. On ramping the field down, significant hysteresis is observed. The intermediate-field Dy spin-flop state does not appear at all. The zero-field polarization is

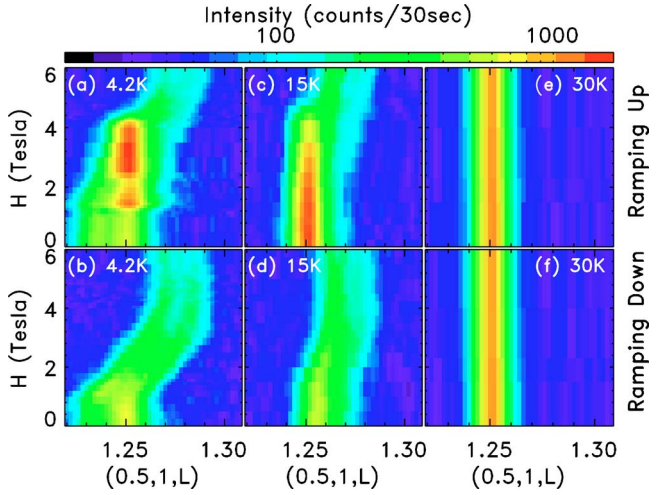

FIG. 2. (Color online) Contour maps of the (0.5,1,L) peak intensity in an applied magnetic field at various temperatures on ramping the field up and then down, as shown in the legend. The temperature protocol is described in the text.

recovered incompletely; its recovery is associated with reappearance of the $C+IC1$ mixed state, and of the Dy (0.5,0,0) order.

By repeating the measurements of Fig. 3 at different temperatures on warming from 4.2 K, we have constructed the magnetic phase diagram of $DyMn_2O_5$ shown in Fig. 4. The diagram contains the C, $IC1(\delta<0)$, $IC2(\delta>0)$, and the $q=(0.5,0,0)$ (Dy AFM) states and several phase-coexistence regions. Regions exhibiting a ferromagnetic signal (FM), most likely due to spin canting, are also shown. The data of Figs. 1 and 3 show that strongly hysteretic dielectric transi-

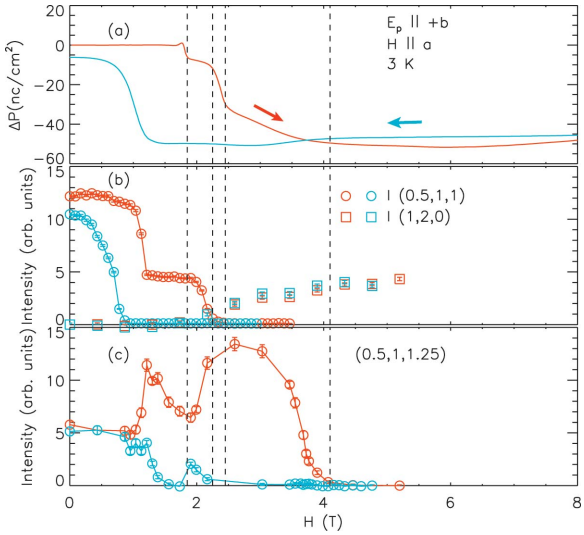

FIG. 3. (Color) (a) Change of the b-axis electric polarization at $T=3$ K in a magnetic field applied along the a axis (from Ref. 7). (b) Intensity of the (0.5,1,1) peak (circles), and of the (1,2,0) peak (squares) vs the a-axis component of the magnetic field H_a at $T=4.2$ K. (c) Intensity at $q=(0.5,1,1.25)$ vs H_a at $T=4.2$ K. In all measurements, the sample was initially cooled in zero magnetic field. The field was ramped up (red symbols), then down (blue symbols).

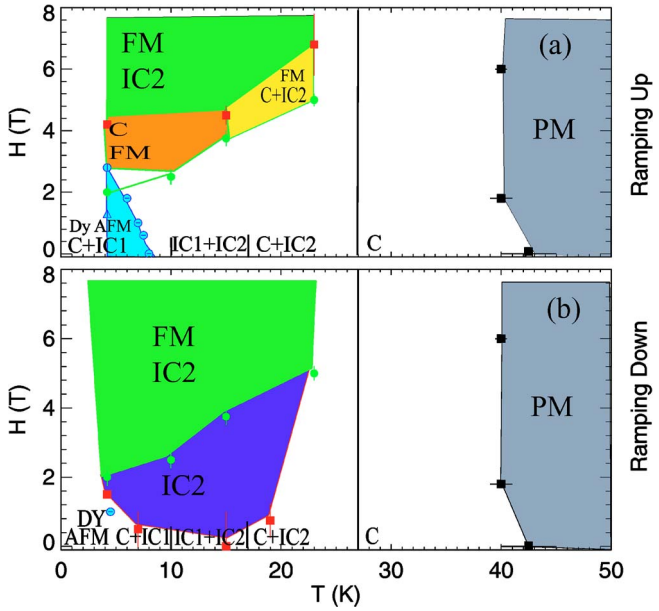

FIG. 4. (Color online) Magnetic phase diagram of $DyMn_2O_2$. The data were taken on warming from $T=4.2$ K, and on subsequent ramping the magnetic field up (a), and then down (b). PM denotes the paramagnetic phase. The other phases are defined in the text.

tions in $DyMn_2O_5$ are associated with the corresponding magnetic transitions. From our data at low temperatures, two scenarios are possible. One is that the material has a multiphase character; the other is that we have a multi-k structure in which multiple wave vectors participate in the ordering. While our data cannot distinguish between these two scenarios, they do show that the presence of several competing ground states is key to understanding the magnetoelectric properties of this material. In particular, for $T>27$ K, where there is only one magnetic phase, with one ordering wave vector, no significant ME effects are found.[7] The complex temperature dependence of the dielectric polarization in $REMn_2O_5$ has previously been ascribed to the presence of two antiparallel FE sublattices, each with its own temperature dependence.[6,7] Our measurements are consistent with this model, provided that the FE sublattices are associated with different coexisting magnetic phases. However, another possibility is that the different spin components couple differently to the polarizations and it is the competition between these different couplings which result in the observed ME properties. Currently, there are several conflicting reports of the FE properties of $DyMn_2O_5$ (Refs. 7 and 11), and therefore it is impossible to deduce the FE properties of the specific magnetic phases by combining these reports with our measurements.

The observed complexity of the magnetic phase diagram results from an intricate interplay of at least five magnetic Mn—Mn interactions in the geometrically frustrated structure of $REMn_2O_5$ (Ref. 9). Indeed, it is well known that coupled magnetic chains, which constitute the primary motif of the Mn sublattice in $REMn_2O_5$, exhibit a variety of nearly degenerate magnetic structures in the presence of competing interactions or magnetoelastic coupling.[15] The presence of multiple ordering wave vectors observed in our experiments is, in fact, a clear signature of competing ground states. Interestingly, the appearance of the electric polarization and the $(0.5,0,0.25+\delta)$ magnetic structure is not dependent on the magnetism of the rare-earth sublattice in $REMn_2O_5$. Indeed, the isostructural YMn_2O_5 also exhibits significant ME effects and possesses similar Mn magnetic structures. However, magnetic fields exceeding 10 T are required to induce any significant ME effect in YMn_2O_5 (Ref. 16). Evidently, coupling of the Mn moments to the large-moment rare-earth ions in $REMn_2O_5$ drives the required fields to significantly lower values. Thus, the basic physics of the ME effects in $REMn_2O_5$ is contained in the magnetic and magnetoelastic interactions within the Mn subsystem, while the coupling to the rare-earth ions is responsible for the low magnetic fields required to induce the magnetic and the dielectric transitions. Summarizing, in $DyMn_2O_5$, magnetic frustration of the Mn lattice coupled to Dy moments results in a magnetic system that shows several magnetic structures, nearly degenerate in energy. The unusual combination of the frustrated magnetic system with strong magnetoelastic coupling is responsible for the intriguing ME effects in $REMn_2O_5$.

This work was supported by the NSF under Grants No. DMR-9986442 and DMR-0093143. M.K. was supported by the National Science Foundation through Grant No. DMR-0306940.

[1] G. A. Smolenskii and I. E. Chupis, Sov. Phys. Usp. **25**, 475 (1982).
[2] H. Schmid, Ferroelectrics **162**, 317 (1994).
[3] R. E. Cohen, J. Phys. Chem. Solids **61**, 139 (2000).
[4] T. Kimura *et al.*, Nature (London) **426**, 55 (2003).
[5] T. Goto *et al.*, Phys. Rev. Lett. **92**, 257201 (2004).
[6] N. Hur *et al.*, Nature (London) **429**, 392 (2004).
[7] N. Hur *et al.*, Phys. Rev. Lett. **93**, 107207 (2004).
[8] S. C. Abrahams and J. L. Bernstein, J. Chem. Phys. **46**, 3776 (1967).
[9] L. C. Chapon *et al.*, Phys. Rev. Lett. **93**, 177402 (2004); G. R. Blake *et al.*, Phys. Rev. B **71**, 214402 (2005).
[10] C. Wilkinson *et al.*, J. Phys. C **14**, 1671 (1981).
[11] D. Higashiyama *et al.*, Phys. Rev. B **70**, 174405 (2004).
[12] I. Kagomiya *et al.*, Ferroelectrics **286**, 167 (2003).
[13] O. Tchernyshyov *et al.*, Phys. Rev. B **68**, 144422 (2003).
[14] Conclusions about spin reorientation are drawn from the analysis of the intensities of up to four $(h+0.5,k,l+0.25+\delta)$ peaks measured in our experiments.
[15] Per Bak, Rep. Prog. Phys. **45**, 587 (1982); N. Ishimura, J. Phys. Soc. Jpn. **54**, 4752 (1985).
[16] Yu. F. Popov *et al.*, J. Exp. Theor. Phys. **96**, 961 (2003).